Dynamics of ethylene groups and hyperfine interactions between donor and anion molecules in λ-type organic conductors studied by ^{69,71}Ga-NMR spectroscopy

N. Yasumura,[1] T. Kobayashi,[1, 2, *] H. Taniguchi,[1] S. Fukuoka,[3] and A. Kawamoto[3]

[1]*Graduate School of Science and Engineering, Saitama University, Saitama, 338-8570, Japan*
[2]*Research and Development Bureau, Saitama University, Saitama 338-8570, Japan*
[3]*Department of Condensed Matter Physics, Graduate School of Science, Hokkaido University, Sapporo 060-0810, Japan*

(Dated: November 10, 2022)

We present the results of ^{69,71}Ga-NMR measurements on an organic antiferromagnet λ-(BEDSe-TTF)$_2$GaCl$_4$ [BEDSe-TTF=bis(ethylenediseleno)tetrathiafulvalene], with comparison to reports on λ-(BETS)$_2$GaCl$_4$ [BETS=bis(ethylenedithio)tetraselenafulvalene] [T. Kobayashi *et al.*, Phys. Rev. B **102**, 235131 (2020)]. We found that the dynamics of two crystallographically independent ethylene groups induce two types of quadrupolar relaxation in the high-temperature region. As the ethylene motion freezes, hyperfine (HF) interactions develop between π spin and Ga nuclear spin below 100 K, and thereby magnetic fluctuations of the π-spin system are detected even from the Ga site. The HF interaction in λ-(BETS)$_2$GaCl$_4$ was more than twice as large as in λ-(BEDSe-TTF)$_2$GaCl$_4$, implying that the short contacts between Cl atoms and the chalcogens of fulvalene part are essential for the transferred HF interaction. We propose that NMR using nuclei in anion layers is useful for studying interlayer interactions in organic conductors, which have not been studied experimentally. In addition, because the mechanism of the transferred HF interaction is considered to be the same as π–d interaction in isostructural Fe-containing λ-type salts, our findings aid in the understanding of their physical properties.

I. INTRODUCTION

Most ET-based organic conductors are regarded as quasi-two-dimensional (Q2D) electronic systems, as well as cuprate and iron-based superconductors, where ET denotes bis(ethylenedithio)tetrathiafulvalene. They often exhibit unconventional superconductivity in the vicinity of magnetically ordered phases [1]. To further understand these Q2D electronic systems, the role of the interlayer interaction has been discussed since long-range ordered states, such as superconductivity and magnetic ordering, require three-dimensional interaction. Electron spin resonance measurements in representative κ-type ET salts suggest that the Fermi liquid and Mott insulating states of these materials are formed below the temperature at which interlayer electron hopping and exchange interaction develop, respectively [2, 3]. The magnetic structures of two κ-type salts have recently been revealed. Although they had been considered to be located in the same antiferromagnetic (AF) phase, their magnetic structures were found to be different each other [4, 5]. It is concluded that the difference in magnetic structure is due to difference in the sign of the interlayer magnetic interaction.

Interlayer interactions not only act between the conducting layers but also act between the conducting and insulating layers when magnetic ions are introduced into the insulating layer. λ-(BETS)$_2$FeCl$_4$ (BETS represents bis(ethylenedithio)tetraselenafulvalene [Fig. 1(a)]) exhibits a field-induced superconductivity above 17 T by the exchange interaction between the conductive

π electron and the localized $3d$ spin of Fe^{3+} [6–8], which is known as π–d interaction. This interaction gives rise to the metal–insulator transition accompanied by AF ordering at zero magnetic fields [9, 10]. In addition, π–d interaction causes unusual multistep magnetization processes in λ-(STF)$_2$FeCl$_4$ and λ-(BEDSe-TTF)$_2$FeCl$_4$ [11, 12], where STF and BEDSe-TTF (noted BEST in Ref. [12]) represent unsymmetrical-bis(ethylenedithio)diselenadithiafulvalene and bis(ethylenediseleno)tetrathiafulvalene [Fig. 1(a)], respectively. These behaviors suggest that interlayer interactions play a crucial role for the various phenomena appearing in Q2D organic systems. However, there are few experimental approaches to evaluate the strength or path of the interlayer interaction.

Meanwhile, in ET-based organic conductors, the dynamics of the ethylene end groups on donor molecules affect the electronic states. In κ-type organic conductors, it has been proposed that a bad metal state is realized at high temperatures because of its dynamics [13, 14]. Particularly in κ-(ET)$_2$Cu[N(CN)$_2$]I, the conformation of the ethylene groups changes the ground state [15, 16]. Moreover, hydrogen bonding between protons of the ethylene groups and the anion has been discussed [17, 18]; therefore, the relationships between the dynamics of ethylene groups and the interlayer interactions should be addressed.

To investigate the interlayer interactions and dynamics of ethylene groups (ethylene motion), nuclear magnetic resonance (NMR) spectroscopy using nuclei in anion layers, "anion NMR", is suggested. Recently, we conducted ^{69,71}Ga-NMR measurements on a superconductor, λ-(BETS)$_2$GaCl$_4$ (hereafter λ-BETS) [19]. In the high-temperature region, quadrupolar relaxation, derived from the translational motion of GaCl$_4^-$, was ob-
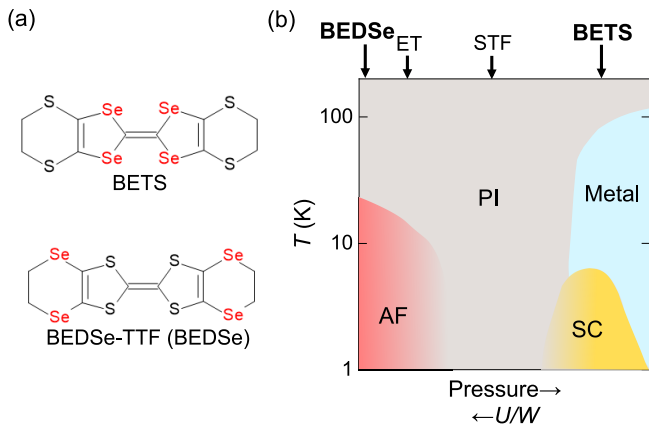
FIG. 1. (a) Molecular structures of BETS and BEDSe-TTF. (b) Temperature-pressure phase diagram of λ-D_2GaCl$_4$ [20, 21]. AF, PI, and SC denote antiferromagnetic, paramagnetic insulating, and superconducting phases, respectively.

served. We suggested that this molecular motion could be induced by the ethylene motion; however, the study from a structural viewpoint is needed to prove this. At low temperatures where the molecular motion freezes, magnetic fluctuation of the electronic system was observed via the transferred hyperfine (HF) interaction between the π spins and Ga nuclei. This fact suggests that anion NMR is useful for evaluating interlayer interactions.

While λ-type salts exhibit physical properties derived from interlayer interactions as seen in λ-D_2FeCl$_4$ (D: donor molecule), their physical properties change by donor molecular substitutions due to the electron correlation effect. In λ-D_2GaCl$_4$, D = ET and BEDSe-TTF salts are antiferromagnetic insulators [20, 22]. D = STF salt is a paramagnetic insulator without long-range ordering [23] and exhibits superconductivity under pressure [24]. While D = BETS salt exhibits semiconducting behavior above 100 K, it becomes a metal and a superconductor below $\sim$ 6 K [25]. These properties can be understood by the universal phase diagram shown in Fig. 1 (b) [20, 21]. Note that D = BETS and other salts exhibit the same semiconducting behavior near room temperature, but the electrical resistivities of them significantly differ at room temperature, e.g., 0.03 Ω cm for D = BETS [26] and 10 Ω cm for D = BEDSe-TTF [27]. The difference in U/W can explain their electrical conductivity [20], where U and W are on-site Coulomb repulsion and bandwidth, respectively. How molecular substitutions change the interlayer interactions along with the electronic correlations is also important for a comprehensive understanding of λ-type salts, including λ-D_2FeCl$_4$. To investigate this, ^{69,71}Ga NMR is an effective probe because it can observe the magnetism of λ-D_2GaCl$_4$ from the same Ga site regardless of donor molecule.

In this study, we report ^{69,71}Ga-NMR measurements on a AF insulator λ-(BEDSe-TTF)$_2$GaCl$_4$ (hereafter λ-

BEDSe) and compare the HF coupling constant of λ-BEDSe with that of a superconductor λ-BETS. We can discuss the path of the interlayer interaction since S and Se atoms in the BETS molecule are exchanged in the BEDSe-TTF molecule, as shown in Fig. 1(a). In addition, x-ray diffraction measurements were conducted to discuss the relationship between the quadrupolar relaxation at high temperatures and the ethylene motion.

II. EXPERIMENTS

Single crystals of λ-BEDSe were synthesized electrochemically [20]. NMR measurements of ^{69}Ga (nuclear spin $I = \frac{3}{2}$, gyromagnetic ratio $^{69}\gamma/2\pi = 10.219$ MHz/T, nuclear quadrupole moment $^{69}Q = 0.171$ barns) and ^{71}Ga ($I = \frac{3}{2}$, $^{71}\gamma/2\pi = 12.984$ MHz/T, $^{71}Q = 0.107$ barns) were performed on the central ($\frac{1}{2} \leftrightarrow -\frac{1}{2}$) transition under the magnetic fields of 6.083 T. We used a moderately crushed polycrystalline sample of about 20 mg, which was randomly oriented with respect to the magnetic field. The spectra were obtained via fast Fourier transformation of the echo signal with a $\frac{\pi}{2}$–π pulse sequence, where the $\frac{\pi}{2}$ pulse length was typically 3 μs. The spin-lattice relaxation time, T_1, was measured using the conventional saturation-recovery method. Single-crystal x-ray diffraction data of λ-BEDSe were collected using a Bruker SMART APEX II ULTRA diffractometer with Mo-Kα radiation ($\lambda = 0.71073$ Å) at the Comprehensive Analysis Center for Science, Saitama University. The crystal structures were solved and refined by SHELXT [28] and SHELXL [29], respectively.

III. RESULTS AND DISCUSSION

A. Spectra

Figure 2 shows ^{69,71}Ga-NMR spectra of λ-BEDSe and λ-BETS [19] at 210 K originating from the central ($\frac{1}{2} \leftrightarrow -\frac{1}{2}$) transition. The spectra with $I = \frac{3}{2}$ can be described by the nuclear spin Hamiltonian as follows:

$$\mathcal{H} = \mathcal{H}_Z + \mathcal{H}_Q$$
$$= -^n\gamma\hbar\boldsymbol{H} \cdot \boldsymbol{I} + \frac{\hbar^n\omega_Q}{6}\left[3I_z^2 - \boldsymbol{I}^2 + \frac{\eta}{2}(I_+^2 + I_-^2)\right], \quad (1)$$

where $n = 69, 71$. $\mathcal{H}_Z$ is the Zeeman interaction: $\hbar$ and $\boldsymbol{H}$ are the reduced Planck constant and external magnetic field, respectively. $\mathcal{H}_Q$ is the quadrupolar interaction: η and ω_Q denotes the asymmetry parameter of electric field gradient (EFG) and the nuclear quadrupolar frequency, respectively. $^n\omega_Q$ is defined as $^n\omega_Q = e\,^nQV_{ZZ}/2\hbar$, where e and V_{ZZ} are the elementary charge and principal axis of the EFG, respectively. The EFG at the Ga site is almost zero because the Ga nucleus in these materials is tetrahedrally coordinated by four Cl$^-$ ions. Thus,
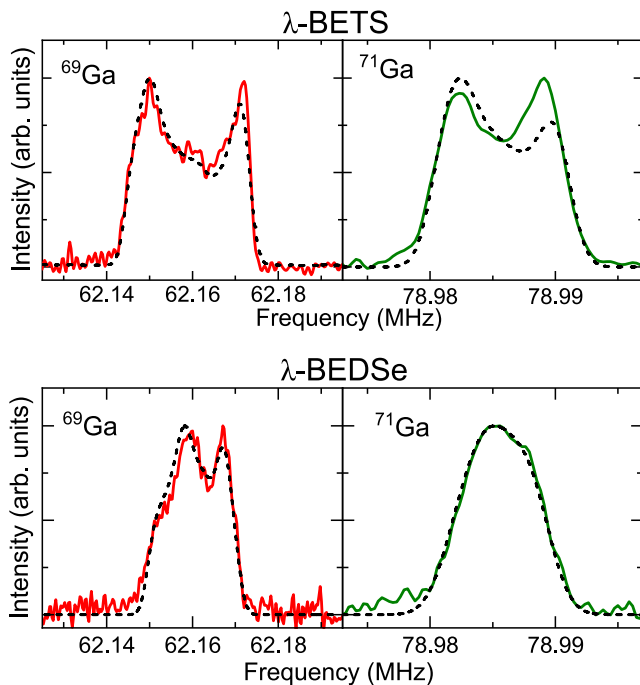
FIG. 2. ^{69,71}Ga-NMR central spectra of λ-BEDSe and λ-BETS [19] at 210 K. Dashed lines are the calculated spectra with parameters listed in Table I.

TABLE I. Parameters of the calculated ^{69,71}Ga-NMR spectra depicted by dashed lines in Fig. 2.

	λ-BEDSe	λ-BETS
$^{69}\omega_{\mathrm{Q}}/2\pi$ (MHz)	1.35	1.73
$^{71}\omega_{\mathrm{Q}}/2\pi$ (MHz)	0.94	1.20
η	0.43	0.17

$\mathcal{H}_{\mathrm{Q}}$ is sufficiently smaller than $\mathcal{H}_{\mathrm{Z}}$. Two peaks were observed in ^{69,71}Ga-NMR spectra of λ-BETS, and the spectral shapes are determined by the powder pattern due to the second-order perturbation effect when $\mathcal{H}_{\mathrm{Q}}$ is treated as a perturbation to $\mathcal{H}_{\mathrm{Z}}$ [19, 30]. The slightly distorted tetrahedral coordination of GaCl$_4^-$ causes the finite EFG at the Ga site.

Although the Ga site of λ-BEDSe is in the same situation as that of λ-BETS, spectral splitting due to second-order perturbation was observed only in ^{69}Ga NMR, implying that the EFG at the Ga site in λ-BEDSe is smaller than that in λ-BETS because the splitting interval is proportional to ω_{Q}^2 [31]. To discuss the difference in the spectra of the two salts quantitatively, we carried out numerical simulation to reproduce them, as shown by the dashed lines in Fig. 2. ^{69,71}Ga-NMR spectra of each salt can be reasonably reproduced by the parameters shown in Table I, where $^n\omega_{\mathrm{Q}} \propto {^nQ}$. In terms of the results of λ-BETS, the parameters are consistent with those obtained from simulation of the overall ^{69}Ga-NMR spec-
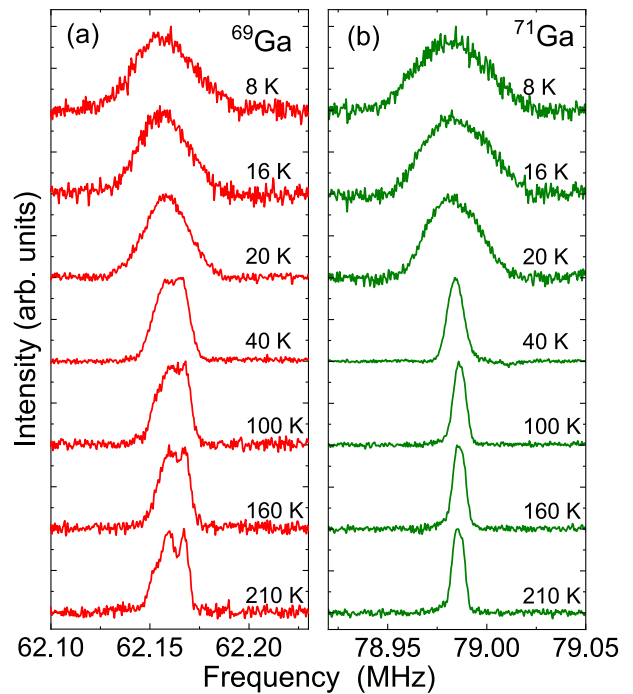

FIG. 3. Central spectra of (a) ^{69}Ga and (b) ^{71}Ga NMR of λ-BEDSe at various temperatures.

trum including satellite peaks at 80 K [19]. When the results of both salts are compared, $^n\omega_{\mathrm{Q}}$ of λ-BEDSe is smaller than that of λ-BETS, resulting in no splitting in the ^{71}Ga-NMR spectra with smaller Q. Reference [32] suggested that the EFG tensor at the tetrahedrally coordinated central atom is sensitive to the arrangement of the surrounding ions. The difference in $^n\omega_{\mathrm{Q}}$ between λ-BETS and λ-BEDSe is only ~ 20 % despite the sensitivity to Cl$^-$ ion arrangement, suggesting that the GaCl$_4^-$ in both salts is almost in the same environment.

Figure 3 shows the temperature evolution of ^{69,71}Ga-NMR spectra of λ-BEDSe. Whereas the spectral shapes are almost unchanged above 40 K, significant line broadening was observed below 20 K. This behavior is understood as the development of the internal magnetic field due to the AF ordering of the π-spin system at $T_{\mathrm{N}} = 22$ K [20]. This observation suggests that ^{69,71}Ga-NMR spectra can detect the static magnetic properties of the π spin system of λ-BEDSe, although the Ga site is far from the π spins.

Gaussian-shaped spectra were observed below 20 K, whereas the spectral shapes above 40 K are dominated by the powder pattern due to the second-order perturbation. To phenomenologically evaluate the linewidth, we estimated the square root of the second moment: $\langle f_{\mathrm{2nd}} \rangle^{1/2} = \left[\int I(f)\,(f - \langle f \rangle)^2\,df / \int I(f)\,df \right]^{1/2}$, where $\langle f \rangle = \int f\,I(f)\,df / \int I(f)\,df$ is the first moment and $I(f)$ is the spectral intensity as a function of frequency f. Figure 4 shows the temperature dependence of $\langle f_{\mathrm{2nd}} \rangle^{1/2}$ of ^{69,71}Ga-NMR spectra, $\langle ^{69,71}f_{\mathrm{2nd}} \rangle^{1/2}$. $\langle ^{69,71}f_{\mathrm{2nd}} \rangle^{1/2}$
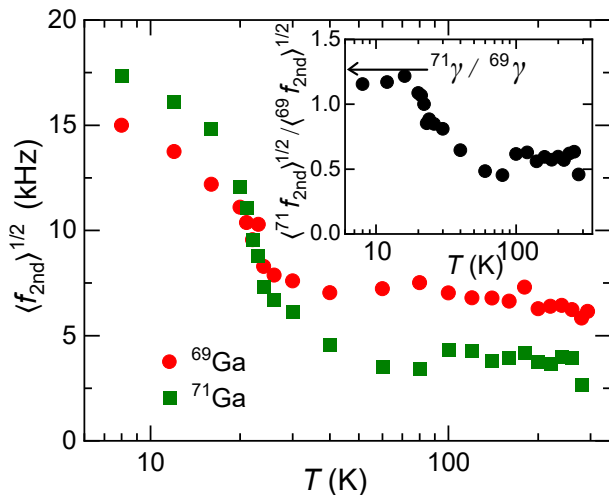
FIG. 4. Second moment $\langle^{69,71}f_{\mathrm{2nd}}\rangle^{1/2}$ of λ-BEDSe as a function of temperature. Inset shows the temperature dependence of the isotopic ratio of $\langle f_{\mathrm{2nd}}\rangle^{1/2}$. The arrow represents the value of $^{71}\gamma\,/\,^{69}\gamma$.

FIG. 5. $^{69,71}T_1^{-1}$ of λ-BEDSe above 100 K as a function of temperature. Inset shows $^{69,71}T_1^{-1}$ of λ-BETS [19]. Solid lines are the fitting curves by Eq. (2) with the fitting parameters listed in Table II.

increase sharply below approximately 40 K owing to the magnetic fluctuation of the π spins. In addition, $\langle^{69}f_{\mathrm{2nd}}\rangle^{1/2}$ is larger than $\langle^{71}f_{\mathrm{2nd}}\rangle^{1/2}$ at high temperatures; however, the relationship is reversed at low temperatures. This indicates that the second moment is dominated by the quadrupolar interaction at high temperatures ($^{69}Q > {}^{71}Q$) and the magnetic interaction at low temperatures ($^{71}\gamma > {}^{69}\gamma$). The inset of Fig. 4 shows that the isotopic ratio of $\langle f_{\mathrm{2nd}}\rangle^{1/2}$ below 18 K is almost identical to $^{71}\gamma/^{69}\gamma$.

In ^{69,71}Ga-NMR spectral measurements, we observed spectra with the typical shapes generated by the finite EFG at the Ga site in the high-temperature region as well as λ-BETS and confirmed the line broadening due to the AF ordering of the π spin system despite the Ga site being far from the π spins. Thus, the spectral study enable us to discuss the static properties of both the EFG and magnetic field at the Ga site.

B. Dynamics of molecular motion in high-temperature region

T_1 measurements allow us to evaluate the magnetic and EFG fluctuations and to distinguish which is dominant using the difference in the properties of the two isotopes. The recovery curves for the central ($\frac{1}{2} \leftrightarrow -\frac{1}{2}$) transition were fitted using the following function; $1 - M(t)/M(\infty) = 0.1\exp[-(t/T_1)^\beta] + 0.9\exp[-(6t/T_1)^\beta]$, where $M(t)$ is the nuclear magnetization at time t after the saturation, $M(\infty)$ is the nuclear magnetization at equilibrium ($t \to \infty$), and β is the stretch exponent. The recovery curves above 100 K were well fitted by the function with $\beta = 1$, whereas β decreased towards T_{N} at
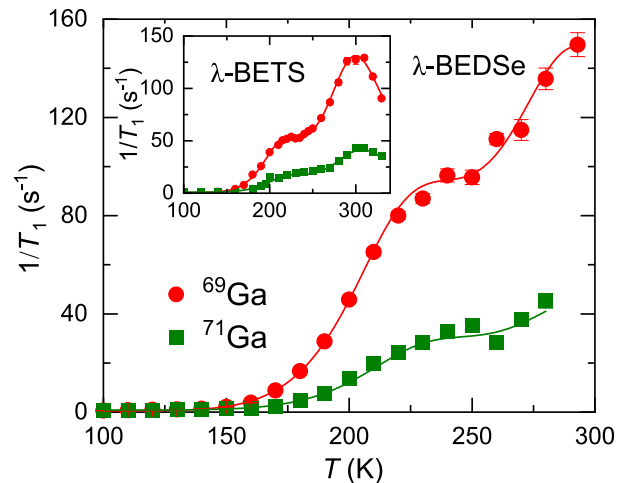
TABLE II. Parameters for $^{69}T_1^{-1}$ above 100 K fitted by Eq. (2).

	λ-BEDSe		λ-BETS	
	$i=1$	$i=2$	$i=1$	$i=2$
$E_{\mathrm{A},i}/k_{\mathrm{B}}$ (10^3 K)	2.0(1)	3.2(7)	1.9(1)	2.9(2)
$\tau_{0,i}$ (10^{-13} s)	4.3(16)	0.5(14)	3.8(17)	1.6(9)
$\langle^{69}\omega_{\mathrm{Q},i}^2\rangle^{1/2}/2\pi$ (kHz)	281(12)	353(8)	215(4)	348(4)
$\langle^{71}\omega_{\mathrm{Q},i}^2\rangle^{1/2}/2\pi$ (kHz)	176(7)	220(5)	134(2)	218(2)
$^{69}T_{1,\mathrm{m}}^{-1}$ (s^{-1})	0.52(7)		0.61(9)	
$^{71}T_{1,\mathrm{m}}^{-1}$ (s^{-1})	0.84(12)		0.98(14)	

low temperatures as discussed in Sec. III C.

Figure 5 shows the temperature dependence of $^{69,71}T_1^{-1}$ (T_1^{-1} of ^{69,71}Ga NMR) of λ-BEDSe above 100 K. $^{69}T_1^{-1}$ is greater than $^{71}T_1^{-1}$ in the high-temperature range and the ratio corresponds to the ratio of Q^2, indicating that the quadrupolar relaxation mechanism is dominant. Above 150 K, $^{69,71}T_1^{-1}$ strongly depend on temperature and exhibit shoulder-like anomalies at around 230 K. Similar behavior was also observed in $^{69,71}T_1^{-1}$ of λ-BETS (inset of Fig. 5) [19], which was explained by the Bloembergen-Purcell-Pound (BPP) formula [33]. We conducted the same analysis with slight modification [34] for $^{69,71}T_1^{-1}$ of λ-BEDSe and λ-BETS. $^nT_1^{-1}$ ($n = 69, 71$) with $I = \frac{3}{2}$ can be written as [30, 35, 36],

$$\frac{1}{^nT_1} = \sum_{i=1,2} \frac{\langle^n\omega_{\mathrm{Q},i}^2\rangle}{50}\frac{\tau_{\mathrm{c},i}}{1 + {}^n\omega_{\mathrm{L}}^2\tau_{\mathrm{c},i}^2} + \frac{1}{^nT_{1,\mathrm{m}}}. \quad (2)$$

$^n\omega_{\mathrm{L}}$ is the Larmor frequency ($^{69}\omega_{\mathrm{L}}/2\pi = 62.16$ MHz and $^{71}\omega_{\mathrm{L}}/2\pi = 78.99$ MHz). An effective root-mean-square
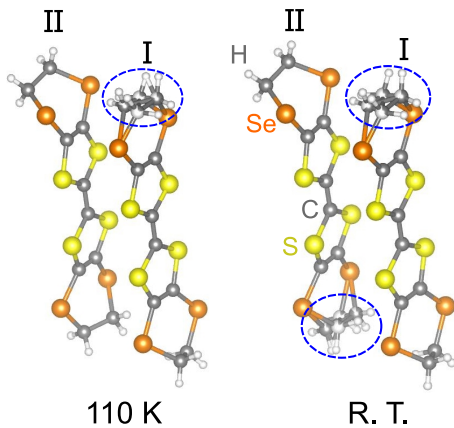
FIG. 6. Donor molecular structures of λ-BEDSe at room temperature (R.T.) and 110 K. The area surrounded by round dashed lines represents the disordered ethylene groups.

FIG. 7. $^{69,71}T_1^{-1}$ (left axis) and $^{13}T_1^{-1}$ (right axis) [20] of λ-BEDSe as a function of temperature.

quadrupole coupling frequency, $\langle^n\omega_{Q,i}^2\rangle^{1/2}$, originates from the modulation of EFG at different equilibrium positions. Since it is proportional to ^nQ, the isotopic ratio of $\langle^{69}\omega_{Q,i}^2\rangle^{1/2}$ to $\langle^{71}\omega_{Q,i}^2\rangle^{1/2}$ is fixed to $^{69}Q/^{71}Q$. $\tau_{c,i}$ is the correlation time described by Arrhenius-type temperature dependence, $\tau_{c,i} = \tau_{0,i}\exp(E_{A,i}/k_BT)$, with a prefactor, $\tau_{0,i}$, activation energy of molecular motion, $E_{A,i}$, and Boltzman constant, k_B. $^nT_{1,m}^{-1}$ is a parameter that originates from the magnetic fluctuation of the π spins in the low-temperature region, where we assumed the constant $^nT_{1,m}^{-1}$, and the ratio $^{71}T_{1,m}^{-1}/^{69}T_{1,m}^{-1} = (^{71}\gamma/^{69}\gamma)^2$. As represented by the solid lines in Fig. 5, the fitting by Eq. (2) reproduces the temperature dependence of $^{69,71}T_1^{-1}$ well, including the reported results of λ-BETS [19]. The obtained fitting parameters for both salts shown in Table II are similar each other, indicating that the quadrupolar relaxation in the high-temperature region can be explained by the same mechanism. This mechanism has been interpreted as the translational motion of GaCl$_4^-$ ions, resulting in the EFG fluctuation at the Ga site [19]. In addition, the nearly identical $E_{A,i}$ and $\tau_{0,i}$ between λ-BETS and λ-BEDSe show that the donor molecular substitution effect on the time scale of the molecular motion is negligible.

In Eq. (2), we assumed two components of the BPP formula ($i = 1, 2$), as shown in Table II. The components of $i = 1$ and 2 correspond to the shoulder-like structures at around 230 K and the further enhancement above 250 K of $^{69,71}T_1^{-1}$ (the latter corresponds to the peak at 300 K in $^{69,71}T_1^{-1}$ of λ-BETS shown in the inset of Fig. 5 [19]), respectively. These results indicate that there are two types of molecular motion with different parameters. Moreover, the translational motion of GaCl$_4^-$ can be induced by the conformational motion of ethylene groups near anion layers, as mentioned in the previous ^{69,71}Ga-NMR study on λ-BETS [19]. To further clarify the relationship between the observed $^{69,71}T_1^{-1}$ and the ethylene motion, x-ray structural
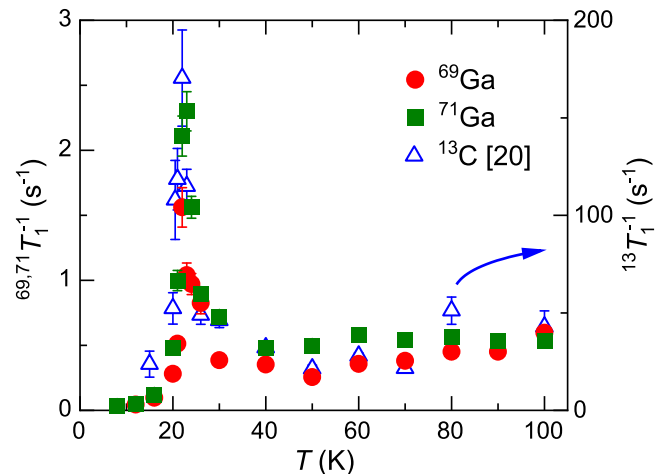
analysis was performed at room temperature (293 K) and 110 K [37]. Figure 6 shows the crystallographically inequivalent molecules I and II extracted from the crystal structure of λ-BEDSe. At room temperature, the ethylene groups at one end of both molecules I and II are disordered, occupying staggered and eclipsed conformations with a ratio of occupancy 0.636(6) : 0.364(6) (molecule I) and 0.131(11) : 0.869(11) (molecule II). At 110 K, molecule I still has disordered sites with the occupancy of 0.797(5) : 0.203(5), whereas molecule II is completely ordered in the eclipsed conformation. Therefore, the ethylene motion of molecule I that remains disordered at lower temperatures is assigned to the $i = 1$ component in Eq. (2), contributing to quadrupolar relaxation on the low-temperature side, and that of molecule II is assigned to $i = 2$ component. This relationship between the two components in the quadrupolar relaxation and the ethylene groups on the two crystallographically independent molecules is considered to hold also in λ-BETS [19].

In addition to the fact that λ-BETS has two types of the ethylene motion [19], the x-ray structural analyses of λ-(BEDSe-TTF)$_2$FeCl$_4$ show that the ethylene groups at the same sites are disordered [12], implying that a similar degree of ethylene motion commonly exists in the λ-type salts. These results will aid our understanding of the mechanisms that cause π–d spin correlations and dielectric anomalies that develop at low temperatures where ethylene motion freezes, as reported for λ-(BETS)$_2$FeCl$_4$ [38, 39].

C. Hyperfine interaction between Ga nuclear spin and π spin

Figure 7 shows the temperature dependence of $^{69,71}T_1^{-1}$ of λ-BEDSe below 100 K. Above 40 K, $^{69,71}T_1^{-1}$ are independent of temperature, but below 40 K, they
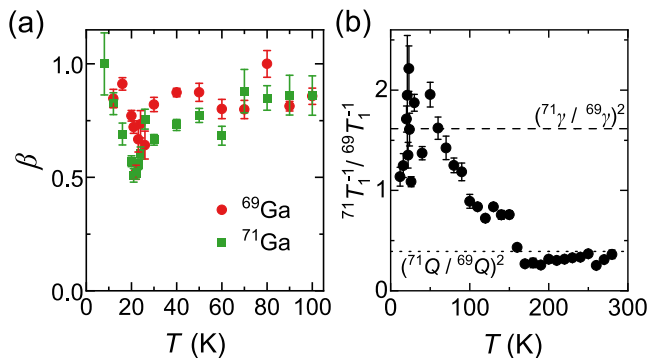
FIG. 8. (a) Stretch exponent β of ^{69,71}Ga NMR below 100 K and (b) $^{71}T_1^{-1}/^{69}T_1^{-1}$ of λ-BEDSe as functions of temperature. Dashed and dotted lines represent the isotopic ratio of γ^2 and Q^2, respectively.

rapidly increase and show the divergent behavior toward T_N = 22 K. The divergence of $^{69,71}T_1^{-1}$ can be attributed to the magnetic transition since the line broadening around T_N is also magnetic, as shown in Fig. 4. In addition, the stretch exponent, β, depends on temperatures below 100 K, as shown in Fig. 8(a). With a decrease in temperature, β decreases from 1 to a minimum at T_N = 22 K. β approaches 1 as the temperature further decreases.

The isotopic ratio of T_1^{-1}, $^{71}T_1^{-1}/^{69}T_1^{-1}$, also confirms that the low-temperature relaxation is due to magnetic fluctuations. Figure 8(b) shows the temperature dependence of $^{71}T_1^{-1}/^{69}T_1^{-1}$. Above 150 K, $^{71}T_1^{-1}/^{69}T_1^{-1}$ values coincide with $\left(^{71}Q/^{69}Q\right)^2$, as mentioned in Sec. III B, depicting the dominance of EFG fluctuation. Below 150 K, $^{71}T_1^{-1}/^{69}T_1^{-1}$ deviates from $\left(^{71}Q/^{69}Q\right)^2$ and approaches $\left(^{71}\gamma/^{69}\gamma\right)^2$, indicating that the magnetic fluctuation becomes dominant as the temperature decreases.

The observed magnetic fluctuation originates from the spin fluctuation of the π spins in the donor layer since the Ga ion is nonmagnetic. The temperature dependence of T_1^{-1} of ^{13}C NMR, $^{13}T_1^{-1}$, is also plotted in Fig. 7 for comparison [20]. Both $^{69,71}T_1^{-1}$ and $^{13}T_1^{-1}$ qualitatively have the same temperature dependence. Thus, the magnetic fluctuation of the π-spin system was probed by ^{69,71}Ga NMR in λ-BEDSe as well as in λ-BETS [19]. These magnetic fluctuations were observed by the suppression of EFG fluctuations as the ethylene motion freezes.

When the magnetic relaxation is due to the spin fluctuation of an electronic system, T_1^{-1} is generally written as follows [40]:

$$\frac{1}{^nT_1} = \frac{2\,^n\gamma^2 k_B T}{\gamma_e^2 \hbar^2} \sum_{\boldsymbol{q}} |^n A_{\boldsymbol{q}}|^2 \frac{\chi''(\boldsymbol{q})}{^n\omega_L}, \quad (3)$$

where γ_e is the gyromagnetic ratio of the electron, $^n A_{\boldsymbol{q}}$ is the wave vector $\boldsymbol{q}$-dependent HF coupling constant, and $\chi''(\boldsymbol{q})$ is the imaginary part of the dynamic susceptibility. Ga sites feel the transferred HF and dipole fields from
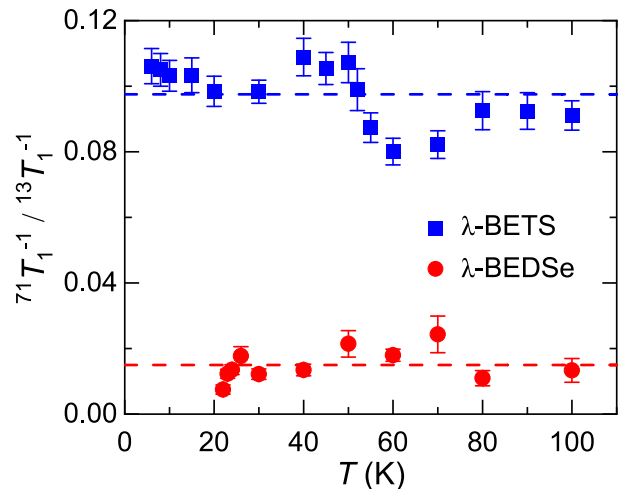

FIG. 9. Temperature dependence of $^{71}T_1^{-1}/^{13}T_1^{-1}$ of λ-BETS and that of λ-BEDSe in the region where the spin fluctuation is dominant. They are obtained from the present and reported data [19, 20, 43]. Dashed lines represent the average values of $^{71}T_1^{-1}/^{13}T_1^{-1}$ of both salts.

the donor sites. First, the dipole field from the donor molecules can be calculated electromagnetically [41] and is of the order of several 10 Oe/μ_B. This estimate can be confirmed from ^{69,71}Ga-NMR spectra in the AF state. Because the external field in the present experiment is larger than the spin-flop field as expected from the typical ET-based antiferromagnet [42], the line broadening of ^{69,71}Ga NMR is dominated by the dipole field. As can be seen in $\langle^{71}f_{2nd}\rangle^{1/2}$ (Fig. 4), the line broadening by AF ordering is $\sim$ 14 kHz, which corresponds to 11 Oe. This is consistent with the calculated value. Next, we compare the calculated HF interaction from the dipole field with experiments. For simplicity, the following discussion uses the results for $^{71}T_1^{-1}$ with larger γ. In $^{71}T_1^{-1}$ and $^{13}T_1^{-1}$, the $\sum_{\boldsymbol{q}} \chi''(\boldsymbol{q})$ part in Eq. (3) should be the same since the same magnetic fluctuation appeared. Therefore,

$$\frac{^{71}T_1^{-1}}{^{13}T_1^{-1}} = \frac{^{71}\gamma^2 \sum_{\boldsymbol{q}} |^{71}A_{\boldsymbol{q}}|^2/^{71}\omega_L}{^{13}\gamma^2 \sum_{\boldsymbol{q}} |^{13}A_{\boldsymbol{q}}|^2/^{13}\omega_L}. \quad (4)$$

Figure 9 shows $^{71}T_1^{-1}/^{13}T_1^{-1}$ below 100 K in the paramagnetic state, where the magnetic fluctuations dominate. As depicted by the dashed line, an average value of $^{71}T_1^{-1}/^{13}T_1^{-1}$ is 0.015(5) in λ-BEDSe, resulting in $(\sum_{\boldsymbol{q}} |^{71}A_{\boldsymbol{q}}|^2/\sum_{\boldsymbol{q}} |^{13}A_{\boldsymbol{q}}|^2)^{1/2}$ = 0.11(2). ^{13}A is approximately $\sim$ 5 kOe/μ_B, referring to the λ-BETS results [43]. Applying the same magnitude of ^{13}A to λ-BEDSe (details below) and neglecting the $\boldsymbol{q}$ dependence of the HF coupling constant, the observed HF coupling constant of ^{71}Ga NMR is estimated to be 5 kOe/$\mu_B \times 0.11$ = 550 Oe/μ_B. This is an order of magnitude larger than the value of the dipole field, indicating that the transferred HF interaction is the dominant as the HF mechanism.

We now discuss the magnitude of the transferred HF

interaction for λ-BETS and λ-BEDSe from the ratio of the values of Eq. (4). All the data used in the following discussion were measured at the same condition, and values other than the HF coupling constant cancel out. We obtained the following equation:

$$\frac{(^{71}T_1^{-1}/^{13}T_1^{-1})_{\mathrm{BETS}}}{(^{71}T_1^{-1}/^{13}T_1^{-1})_{\mathrm{BEDSe}}}$$
$$\approx \frac{(^{71}A/^{13}A)_{\mathrm{BETS}}^2}{(^{71}A/^{13}A)_{\mathrm{BEDSe}}^2} \approx \frac{^{71}A_{\mathrm{BETS}}^2}{^{71}A_{\mathrm{BEDSe}}^2}, \tag{5}$$

where the donor molecules are indicated as subscripts. The donor molecular substitution effect on ^{13}A was ignored in the latter approximation since λ-D_2GaCl$_4$ are isostructural and the local environments around ^{13}C nucleus are similar. Actually, $^{13}A_{\mathrm{STF}}$ and $^{13}A_{\mathrm{BETS}}$ are of the same order [23, 43], where $^{13}A_{\mathrm{STF}}$ is the HF coupling constant in λ-(STF)$_2$GaCl$_4$. Therefore, Eq. (5) allows us to compare the magnitude of the HF interaction between λ-BETS and λ-BEDSe from T_1^{-1} measurements. As shown in Fig. 9, the average values were obtained as $(^{71}T_1^{-1}/^{13}T_1^{-1})_{\mathrm{BETS}} = 0.098(9)$ and $(^{71}T_1^{-1}/^{13}T_1^{-1})_{\mathrm{BEDSe}} = 0.015(5)$, resulting in $^{71}A_{\mathrm{BETS}}/^{71}A_{\mathrm{BEDSe}} = 2.6(4)$. This result implies that the magnitude of the transferred HF interaction in λ-BETS is more than two times larger than that in λ-BEDSe. The difference in the magnitudes between λ-BETS and λ-BEDSe suggests that the proton-Cl contacts are not dominant for the transferred HF interaction.

The variation in physical properties due to the donor molecular substitution in λ-D_2GaCl$_4$ has been discussed in terms of chemical pressure effect [21], with λ-BEDSe compound located at the most negative position on the pressure axis (Fig. 1(b)) [20]. Our findings indicate that replacing BETS or STF molecules with BEDSe-TTF molecule causes negative-pressure effect on not only intralayer but also interlayer interactions, which may be necessary for a comprehensive understanding of their physical properties.

Some Se/S–Cl contacts shorter than van der Waals distances (Se–Cl: 3.7 Å, S–Cl: 3.6 Å [44]) exist in λ-BETS [20, 26] and λ-BEDSe, as shown in Fig. 10, which significantly contribute to the transferred HF interaction. The short Se–Cl contact would contribute more to the interaction than the S–Cl contact since the atomic radius of Se is larger than that of S. Although the number of short Se–Cl contacts in λ-BEDSe is greater than that in λ-BETS with an extremely short Se–Cl contact of $d_2 = 3.2601(8)$ Å, this study demonstrated that the transferred HF interaction of λ-BEDSe is smaller than that of λ-BETS. Therefore, the paths through the inner chalcogens and Cl are more essential for the transferred HF interaction. The inner chalcogens in the ET molecule have larger coefficients of the highest occupied molecular orbital proportional to the electron density than the outer chalcogens [45], which could be why the paths through the inner chalcogen and Cl are crucial.
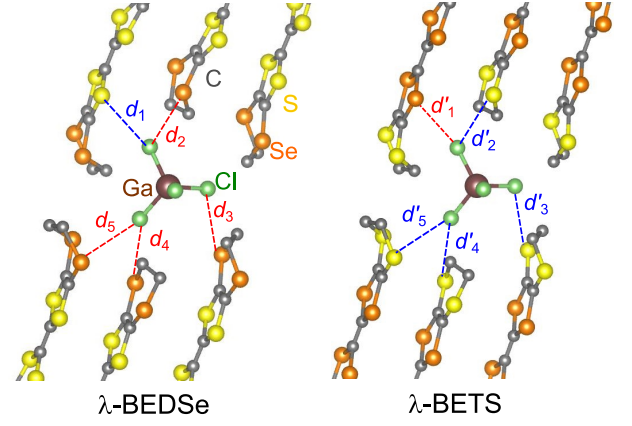

FIG. 10. Short contacts between Cl and chalcogens in λ-BEDSe and λ-BETS. Blue (red) dashed lines represent short contacts between S (Se) and Cl within the van der Waals distances of 3.6 Å (S–Cl) and 3.7 Å (Se–Cl): λ-BEDSe; $d_1 = 3.5978(13)$ Å, $d_2 = 3.2601(8)$ Å, $d_3 = 3.5230(11)$ Å, $d_4 = 3.5139(9)$ Å, $d_5 = 3.6301(8)$ Å, λ-BETS; $d_1' = 3.5144(12)$ Å, $d_2' = 3.4084(12)$ Å, $d_3' = 3.5699(15)$ Å, $d_4' = 3.6006(14)$ Å, $d_5' = 3.5540(12)$ Å.

As discussed above, the coupling constants between π electrons and the Ga nuclear spins were obtained by combining the results of ^{69,71}Ga-NMR and ^{13}C-NMR measurements. This enables us to explain the coupling between the conduction layers via the anion layer although such a discussion has been difficult until now. In addition to the difference in the electronic states between λ-BEDSe and λ-BETS, this study reveals that the interlayer interaction is smaller in λ-BEDSe. Thus, we demonstrate that anion NMR experiment is a powerful method for investigating the interlayer interactions. The contribution of such interactions has also been suggested for κ-type organic antiferromagnets. Since the κ-(ET)$_2$Cu[N(CN)$_2$]Cl and deuterated κ-(ET)$_2$Cu[N(CN)$_2$]Br salts are isostructural, the same magnetic structure is expected from the anisotropy resulting from dipole interactions. However, magnetization measurements and numerical simulations have recently revealed that the magnetic structures are different between them [4, 5]. In organic magnets, which are similar to the Heisenberg spin systems, interlayer coupling could be particularly important for three-dimensional order. Anion NMR will be helpful for clarifying this issue and also the development of interlayer coupling upon cooling [2, 3].

Finally, we discuss the relationship between the transferred HF interaction in λ-D_2GaCl$_4$ and the π–d interaction in λ-D_2FeCl$_4$. The transferred HF interaction is between the π spin and the Ga nuclear spin, whereas the π–d interaction is between the π spin and the $3d$ spin of Fe^{3+} ion. This study experimentally revealed the importance of the path through the inner chalcogen and Cl for the transferred HF interactions. Mori and

Katsuhara also reported that the interaction via short Se–Cl contacts has the largest contribution to the π–d interaction in λ-(BETS)$_2$FeCl$_4$ from the calculation of the intermolecular overlap integrals [46]. Therefore, the transferred HF and π–d interactions can be attributed to the same mechanism. The reported λ-D_2FeCl$_4$ salts are D = BETS, STF, and BEDSe-TTF, which are antiferromagnets with T_N = 8.5, 16, and 25 K, respectively [10–12]. Among them, λ-(BETS)$_2$FeCl$_4$ is expected to have the largest π–d interaction, and λ-(BEDSe-TTF)$_2$FeCl$_4$ is expected to have the smallest π–d interaction due to the weak interaction between inner S and Cl [12]. Magnetic susceptibility of λ-(BEDSe-TTF)$_2$FeCl$_4$ does not show an anisotropy [12] as well as that of λ-(BETS)$_2$FeBr$_x$Cl$_{4-x}$ for $0.3 < x < 0.5$ [47], whereas those of λ-(BETS)$_2$FeCl$_4$ and λ-(STF)$_2$FeCl$_4$ show an anisotropy below 8 K [10, 48]. Akutsu et $al.$ claimed that the π–d interaction in λ-(BETS)$_2$FeBr$_x$Cl$_{4-x}$ for $0.3 < x < 0.5$ is weaker than that in λ-(BETS)$_2$FeCl$_4$ [47]. Thus, λ-(BEDSe-TTF)$_2$FeCl$_4$ has been referred to as a weaker π–d system, which is consistent with our findings.

IV. SUMMARY

We performed ^{69,71}Ga-NMR and x-ray diffraction measurements on an organic antiferromagnet, λ-BEDSe. The spectral measurements revealed a powder pattern due to finite EFG at high temperatures and a spectral broadening due to AF ordering at low temperatures, indicating that the static nature of EFG and magnetic fields can be detected even by NMR at Ga sites far from the electron system. In the T_1 measurements, we observed the quadrupolar relaxation described by the BPP formula with two components in the high-temperature re-

gion. By x-ray structural analysis, it was revealed that the two components were assigned to the two crystallographically independent ethylene groups. In the low-temperature region where the ethylene motion freezes, the magnetic fluctuation of the π-spin system was observed through the transferred HF interaction between the π spin and the Ga nuclear spin, as in the case of λ-BETS. We discovered that λ-BETS had a lager transferred HF interaction than λ-BEDSe. This finding enables us to conclude that the short contacts between the chalcogens of the fulvalene part of the donor molecules and the Cl of anion molecules are the most significant contributors to this interaction. The transferred HF interaction in λ-D_2GaCl$_4$ and the π–d interaction in the isostructural λ-D_2FeCl$_4$ can be derived from the same path. Therefore, we also evaluated the π–d interaction in the λ-type π–d system. Present study reveals that anion NMR measurement is an effective tool for studying the interlayer interaction for which experimental approaches are limited in Q2D organic conductors.

[1] K. H. Bennemann and J. B. Ketterson, eds., *Superconductivity* (Springer, Berlin, 2008).

[2] Á. Antal, T. Fehér, E. Tátrai-Szekeres, F. Fülöp, B. Náfrádi, L. Forró, and A. Jánossy, Pressure and temperature dependence of interlayer spin diffusion and electrical conductivity in the layered organic conductors κ-(BEDT-TTF)$_2$Cu[N(CN)$_2$]X (X = Cl, Br), Physical Review B **84**, 075124 (2011).

[3] Á. Antal, T. Fehér, B. Náfrádi, L. Forró, and A. Jánossy, Magnetic fluctuations above the Néel temperature in κ-(BEDT-TTF)$_2$Cu[N(CN)$_2$]Cl, a quasi-2D Heisenberg antiferromagnet with Dzyaloshinskii–Moriya interaction, physica status solidi (b) **249**, 1004 (2012).

[4] R. Ishikawa, H. Tsunakawa, K. Oinuma, S. Michimura, H. Taniguchi, K. Satoh, Y. Ishii, and H. Okamoto, Zero-Field Spin Structure and Spin Reorientations in Layered Organic Antiferromagnet, κ-(BEDT-TTF)$_2$Cu[N(CN)$_2$]Cl, with Dzyaloshinskii–Moriya Interaction, Journal of the Physical Society of Japan **87**,

064701 (2018).

[5] K. Oinuma, N. Okano, H. Tsunakawa, S. Michimura, T. Kobayashi, H. Taniguchi, K. Satoh, J. Angel, I. Watanabe, Y. Ishii, H. Okamoto, and T. Itou, Spin structure at zero magnetic field and field-induced spin reorientation transitions in a layered organic canted antiferromagnet bordering a superconducting phase, Physical Review B **102**, 035102 (2020).

[6] S. Uji, H. Shinagawa, T. Terashima, T. Yakabe, Y. Terai, M. Tokumoto, A. Kobayashi, H. Tanaka, and H. Kobayashi, Magnetic-field-induced superconductivity in a two-dimensional organic conductor, Nature **410**, 908 (2001).

[7] L. Balicas, J. S. Brooks, K. Storr, S. Uji, M. Tokumoto, H. Tanaka, H. Kobayashi, A. Kobayashi, V. Barzykin, and L. P. Gor'kov, Superconductivity in an Organic Insulator at Very High Magnetic Fields, Physical Review Letters **87**, 067002 (2001).

[8] S. Uji and J. S. Brooks, Magnetic-Field-Induced Superconductivity in Organic Conductors, Journal of the Phys-

ical Society of Japan **75**, 051014 (2006).

[9] A. Kobayashi, T. Udagawa, H. Tomita, T. Naito, and H. Kobayashi, New Organic Metals Based on BETS Compounds with MX_4^- Anions (BETS = bis(ethylenedithio)tetraselenafulvalene; M = Ga, Fe, In; X = Cl, Br), Chemistry Letters **22**, 2179 (1993).

[10] M. Tokumoto, T. Naito, H. Kobayashi, A. Kobayashi, V. Laukhin, L. Brossard, and P. Cassoux, Magnetic anisotropy of organic conductor λ-(BETS)$_2$FeCl$_4$, Synthetic Metals **86**, 2161 (1997).

[11] S. Fukuoka, M. Sawada, T. Minamidate, N. Matsunaga, K. Nomura, Y. Ihara, A. Kawamoto, Y. Doi, M. Wakeshima, and Y. Hinatsu, Multistep Development of the Hyperfine Fields in λ-(BEDT-STF)$_2$FeCl$_4$ Studied by Mössbauer Spectroscopy, Journal of the Physical Society of Japan **87**, 093705 (2018).

[12] R. Saito, Y. Iida, T. Kobayashi, H. Taniguchi, N. Matsunaga, S. Fukuoka, and A. Kawamoto, Magnetic state in the quasi-two-dimensional organic conductor λ-(BEST)$_2$FeCl$_4$ and the path of π–d interaction, Physical Review B **105**, 165115 (2022).

[13] Y. Kuwata, M. Itaya, and A. Kawamoto, Low-frequency dynamics κ-(BEDT-TTF)$_2$Cu(NCS)$_2$ observed by ^{13}C NMR, Physical Review B **83**, 144505 (2011).

[14] M. Matsumoto, Y. Saito, and A. Kawamoto, Molecular motion and high-temperature paramagnetic phase in κ-(BEDT-TTF)$_2$Cu[N(CN)$_2$]Cl, Physical Review B **90**, 115126 (2014).

[15] T. Naito, H. Takeda, Y. Matsuzawa, M. Kurihara, A. Yamada, Y. Nakamura, and T. Yamamoto, Organic charge transfer complex at the boundary between superconductors and insulators: critical role of a marginal part of the conduction pathways, Materials Advances **3**, 1506 (2022).

[16] T. Kobayashi, A. Suzuta, K. Tsuji, Y. Ihara, and A. Kawamoto, Inhomogeneous electronic state of organic conductor κ-(BEDT-TTF)$_2$Cu[N(CN)$_2$]I studied by ^{13}C NMR spectroscopy, Physical Review B **100**, 195115 (2019).

[17] P. Alemany, J.-P. Pouget, and E. Canadell, Essential role of anions in the charge ordering transition of α-(BEDT-TTF)$_2$I$_3$, Physical Review B **85**, 195118 (2012).

[18] J.-P. Pouget, P. Alemany, and E. Canadell, Donor–anion interactions in quarter-filled low-dimensional organic conductors, Materials Horizons **5**, 590 (2018).

[19] T. Kobayashi, K. Tsuji, A. Ohnuma, and A. Kawamoto, Selective observation of spin and charge dynamics in an organic superconductor λ-(BETS)$_2$GaCl$_4$ using ^{69,71}Ga NMR measurements, Physical Review B **102**, 235131 (2020).

[20] A. Ito, T. Kobayashi, D. P. Sari, I. Watanabe, Y. Saito, A. Kawamoto, H. Tsunakawa, K. Satoh, and H. Taniguchi, Antiferromagnetic ordering of organic Mott insulator λ-(BEDSe-TTF)$_2$GaCl$_4$, Physical Review B **106**, 045114 (2022).

[21] H. Mori, T. Okano, M. Kamiya, M. Haemori, H. Suzuki, S. Tanaka, Y. Nishio, K. Kajita, and H. Moriyama, Bandwidth and band filling control in organic conductors, Physica C: Superconductivity **357-360**, 103 (2001).

[22] Y. Saito, S. Fukuoka, T. Kobayashi, A. Kawamoto, and H. Mori, Antiferromagnetic Ordering in Organic Conductor λ-(BEDT-TTF)$_2$GaCl$_4$ Probed by ^{13}C NMR, Journal of the Physical Society of Japan **87**, 013707 (2018).

[23] Y. Saito, H. Nakamura, M. Sawada, T. Yamazaki, S. Fukuoka, N. Matsunaga, K. Nomura, M. Dressel, and A. Kawamoto, Disordered quantum spin state in the stripe lattice system consisting of triangular and square tilings, arXiv:1910.09963 (2019).

[24] T. Minamidate, Y. Oka, H. Shindo, T. Yamazaki, N. Matsunaga, K. Nomura, and A. Kawamoto, Superconducting Phase in λ-(BEDT-STF)$_2$GaCl$_4$ at High Pressures, Journal of the Physical Society of Japan **84**, 063704 (2015).

[25] H. Kobayashi, H. Tomita, T. Udagawa, T. Naito, and A. Kobayashi, New organic superconductor, λ-(BETS)$_2$GaCl$_4$ and metal–insulator transition of BETS conductor with magnetic anions (BETS = bis(ethlenedithio)tetraselenafulvalene), Synthetic Metals **70**, 867 (1995).

[26] H. Tanaka, A. Kobayashi, A. Sato, H. Akutsu, and H. Kobayashi, Chemical Control of Electrical Properties and Phase Diagram of a Series of λ-Type BETS Superconductors, λ-(BETS)$_2$GaBr$_x$Cl$_{4-x}$, Journal of the American Chemical Society **121**, 760 (1999).

[27] H. B. Cui, S. Otsubo, Y. Okano, and H. Kobayashi, Structural and Physical Properties of λ-(BEST)$_2$MCl$_4$ (BEST = Bis(ethylenediseleno)tetrathiafulvalene; M = Fe, Ga) and Analogous Magnetic Organic Conductor, Chemistry Letters **34**, 254 (2005).

[28] G. M. Sheldrick, SHELXT–Integrated space-group and crystal-structure determination, Acta Crystallographica Section A Foundations and Advances **71**, 3 (2015).

[29] G. M. Sheldrick, Crystal structure refinement with SHELXL, Acta crystallographica. Section C, Structural chemistry **71**, 3 (2015).

[30] A. A. Abragam, *The principles of Nuclear Magnetism* (Oxford University Press, Oxford, 1961).

[31] M. Cohen and F. Reif, Quadrupole Effects in Nuclear Magnetic Resonance Studies of Solids, Solid State Physics **5**, 321 (1957).

[32] R. W. Schurko, S. Wi, and L. Frydman, Dynamic Effects on the Powder Line Shapes of Half-Integer Quadrupolar Nuclei: A Solid-State NMR Study of XO_4^- Groups, The Journal of Physical Chemistry A **106**, 51 (2002).

[33] N. Bloembergen, E. M. Purcell, and R. V. Pound, Relaxation Effects in Nuclear Magnetic Resonance Absorption, Physical Review **73**, 679 (1948).

[34] We added the $4\tau_{c,i}/(1 + 4^n\omega_L^2\tau_{c,i}^2)$ term in Eq. (2) in our previous discussion in Ref. [19], but this is not correct when considering the physical picture. For example, when the ethylene motion is observed in ^{1}H-NMR, this term exists owing to dipole interactions. In this study, the relaxation is due to the interaction between the EFG and the nuclear spins of Ga and is discussed using Eq. (2).

[35] H. W. Spiess, Rotation of molecules and nuclear spin relaxation, in *Dynamic NMR Spectroscopy* (Springer Berlin Heidelberg, Berlin, Heidelberg, 1978) pp. 55–214.

[36] A. Avogadro, F. Tabak, M. Corti, and F. Borsa, ^{11}B spin-lattice relaxation and disorder modes in ionic glassy conductors (AgI)$_x$(Ag$_2$O·nB$_2$O$_3$)$_{1-x}$, Physical Review B **41**, 6137 (1990).

[37] The crystallographic data for λ-BEDSe (C$_{20}$H$_{16}$S$_8$Se$_8$GaCl$_4$, M = 1356.01): T = 293 K; triclinic, $P\bar{1}$, a = 16.3944(14) Å, b = 18.2469(16) Å, c = 6.7223(6) Å, α = 97.1920(10)°, β = 97.8280(10)°, γ = 112.2740(10)°, V = 1808.9(3) Å^3, D_{calc} = 2.490 (g/cm^3), μ (Mo-Kα) = 9.584 mm^{-1}, F_{000} = 1270, θ_{max} = 29.163°, Number of unique reflections = 8827, R_{int} = 0.0347, $R_1 = \sum ||F_0 - |F_c||/ \sum |F_0| = 0.0364 [I >$

$2\sigma(I)$], $wR_2 = [\sum w(|F_0| - |F_c|)^2 / \sum w|F_0|^2]^{1/2} = 0.0928$ (all data), GOF (goodness of fit) = 1.056, CCDC (Cambridge Crystallographic Data Centre) No. 2192131. $T = 110$ K; triclinic, $P\bar{1}$, $a = 16.1260(14)$ Å, $b = 18.1099(15)$ Å, $c = 6.6519(6)$ Å, $\alpha = 97.3970(10)°$, $\beta = 97.1540(10)°$, $\gamma = 111.8860(10)°$, $V = 1755.9(3)$ Å^3, $D_{calc} = 2.565$, μ(Mo-Kα) = 9.874 mm^{-1}, $F_{000} = 1270$, $\theta_{max} = 29.154°$, Number of unique reflections = 8593, $R_{int} = 0.0253$, $R_1 = 0.0256$ [$I > 2\sigma(I)$], $wR_2 = 0.0609$ (all data), GOF= 1.066, CCDC No. 2192130.

[38] T. Lee, Y. Oshima, H. Cui, and R. Kato, Detailed X-band Studies of the π–d Molecular Conductor λ-(BETS)$_2$FeCl$_4$: Observation of Anomalous Angular Dependence of the g-value, Journal of the Physical Society of Japan **87**, 114702 (2018).

[39] H. Matsui, H. Tsuchiya, E. Negishi, H. Uozaki, Y. Ishizaki, Y. Abe, S. Endo, and N. Toyota, Anomalous Dielectric Response in the π–d Correlated Metallic State of λ-(BEDT-TSF)$_2$FeCl$_4$, Journal of the Physical Society of Japan **70**, 2501 (2001).

[40] T. Moriya, The Effect of Electron-Electron Interaction on the Nuclear Spin Relaxation in Metals, Journal of the Physical Society of Japan **18**, 516 (1963).

[41] Assuming that there is a paramagnetic moment of $1\mu_B$/dimer, which is distributed to each atom by the square of the highest occupied molecular orbital coefficient of BEDSe-TTF [20], dipole field D at the Ga site can be calculated from $D = \sum_i (\boldsymbol{\mu}/r_i^3 - (\boldsymbol{\mu} \cdot \boldsymbol{r}_i)\boldsymbol{r}_i/r_i^5)$, with $\boldsymbol{r}_i \equiv \boldsymbol{R}_i - \boldsymbol{R}_0$ and $r_i \equiv |\boldsymbol{r}_i|$. Here, $\boldsymbol{\mu}$ is the distributed moment on each atom of the BEDSe-TTF molecule, $\boldsymbol{R}_i$ and $\boldsymbol{R}_0$ are position vectors of dipole moment on each atom and Ga atom, respectively. As a result, the dipole field tensor for an arbitrary moment direction derived from BEDSe-TTF molecules in the range of ± 10 unit cells is,

$$\begin{pmatrix} D_{xx} & D_{xy} & D_{xz} \\ D_{yx} & D_{yy} & D_{yz} \\ D_{zx} & D_{zy} & D_{zz} \end{pmatrix} = \begin{pmatrix} -9.2 & -11.4 & 0.8 \\ -11.4 & 92.7 & 18.4 \\ 0.8 & 18.4 & -83.5 \end{pmatrix} \text{Oe}/\mu_B,$$

where the coordinate system is defined by $\boldsymbol{x} \parallel \boldsymbol{a}$, $\boldsymbol{y} \parallel (\boldsymbol{a} \times \boldsymbol{b}) \times \boldsymbol{a}$, $\boldsymbol{z} \parallel \boldsymbol{a} \times \boldsymbol{b}$.

[42] H. Taniguchi, M. Miyashita, K. Uchiyama, R. Sato, Y. Ishii, K. Satoh, N. Môri, M. Hedo, and Y. Uwatoko, High-Pressure Study up to 9.9 GPa of Organic Mott Insulator, β'-(BEDT-TTF)$_2$AuCl$_2$, Journal of the Physical Society of Japan **74**, 1370 (2005).

[43] T. Kobayashi and A. Kawamoto, Evidence of antiferromagnetic fluctuation in the unconventional superconductor λ-(BETS)$_2$GaCl$_4$ by ^{13}C NMR, Physical Review B **96**, 125115 (2017).

[44] S. S. Batsanov, Van der Waals Radii of Elements, Inorganic materials **37**, 871 (2001).

[45] T. Mori, A. Kobayashi, Y. Sasaki, H. Kobayashi, G. Saito, and H. Inokuchi, The Intermolecular Interaction of Tetrathiafulvalene and Bis(ethylenedithio)tetrathiafulvalene in Organic Metals. Calculation of Orbital Overlaps and Models of Energyband Structures, Bulletin of the Chemical Society of Japan **57**, 627 (1984).

[46] T. Mori and M. Katsuhara, Estimation of π–d Interactions in Organic Conductors Including Magnetic Anions, Journal of the Physical Society of Japan **71**, 826 (2002).

[47] H. Akutsu, K. Kato, E. Ojima, H. Kobayashi, H. Tanaka, A. Kobayashi, and P. Cassoux, Coupling of metal-insulator and antiferromagnetic transitions in the highly correlated organic conductor incorporating magnetic anions, Physical Review B **58**, 9294 (1998).

[48] T. Minamidate, H. Shindo, Y. Ihara, A. Kawamoto, N. Matsunaga, and K. Nomura, Role of the d-d interaction in the antiferromagnetic phase of λ-(BEDT-STF)$_2$FeCl$_4$, Physical Review B **97**, 104404 (2018).

[49] K. Momma and F. Izumi, VESTA 3 for three-dimensional visualization of crystal, volumetric and morphology data, Journal of Applied Crystallography **44**, 1272 (2011).

[50] https://www.ccdc.cam.ac.uk/structures/.